J. Phys. B: Atom. Molec. Phys. **13** (1980) 1249–1267. Printed in Great Britain

Absolute ionisation cross sections for electron impact in rare gases

P Nagy, A Skutlartz and V Schmidt

Fakultät für Physik der Universität Freiburg, D-7800 Freiburg, West Germany

Received 22 June 1979, in final form 5 November 1979

Abstract. Absolute ionisation cross sections $\sigma^{n+}(n = 1, 2, 3)$ for electron impact (with energies between 0·5 and 5·0 keV) with rare gases have been determined by a direct method. The values are generally in close agreement with the results of Schram *et al.* A comparison with other experimental data and to some theoretical calculations is given.

1. Introduction

Electron impact ionisation of atoms is a fundamental process from both the experimental and the theoretical point of view. To describe the total ionisation cross sections, two expressions are used which have to be distinguished, σ_{ion} and $\sigma_{\text{gross ion}}$. Both quantities derive from the cross section σ^{n+} for the occurrence of ions with charge n: $\sigma_{\text{ion}} = \Sigma\sigma^{n+}$ and $\sigma_{\text{gross ion}} = \Sigma n\sigma^{n+}$. The present investigation gives σ^{n+} directly.

The electron impact ionisation cross sections are of interest in studies of the penetration of matter by charged particles, and they are of basic importance for theoretical calculations. During the last few years the theoretical aspect was developed in two directions which are beyond the usual comparison of a direct theoretical calculation of ionisation cross sections with experimental data. One method is based on powerful sum rules for the total inelastic scattering cross section $\sigma_{\text{tot, inel}}$ and the excitation cross section σ_{exc}. Their difference gives σ_{ion} (cf Inokuti *et al* 1967, Inokuti 1971, Kim and Inokuti 1971, Saxon 1973, Kim *et al* 1973, Eggarter 1975). The other theoretical treatment is the dispersion-relation analysis of electron–atom scattering (Bransden and McDowell 1969, 1970, de Heer *et al* 1976). For this analysis accurate values of the total scattering cross section σ_{tot} are very important (cf de Heer and Jansen 1977, de Heer *et al* 1979) whereby $\sigma_{\text{tot}} = \sigma_{\text{exc}} + \sigma_{\text{ion}} + \sigma_{\text{el}}$ where σ_{el} is the total elastic scattering cross section.

Unfortunately, the experimental situation for reliable absolute values of σ^{n+}, σ_{ion} and $\sigma_{\text{gross ion}}$ has not been very satisfactory because the available data sets do not agree within their experimental errors, e.g. at 1 keV electron energy the data for He of different experimental groups deviate by more than 20% (compare also the compilation of Kieffer and Dunn 1966). This spread in the experimental data has made a critical comparison with the results of different theoretical approaches rather difficult. For example, theories which are based on sum rule relations seemed to support the $\sigma_{\text{gross ion}}$ data of Smith (1930) for He, Ne and Ar (Kim and Inokuti 1971, Saxon 1973, Eggarter 1975). Those experimental data belong to the set of cross sections with the highest values.

0022-3700/80/061249+19$01.50

In order to improve the experimental situation we decided to modify our charge analysing system (Schmidt *et al* 1976a,b) for an absolute determination of the ionisation cross sections σ^{n+} and therefore also of σ_{ion}. This experimental arrangement and its results will be described.

2. Experimental details

2.1. Apparatus

The main parts of the apparatus can be seen from figure 1. They have been already described earlier in detail (Schmidt *et al* 1976a). Therefore only those modifications will be given which are important for the absolute measurement.

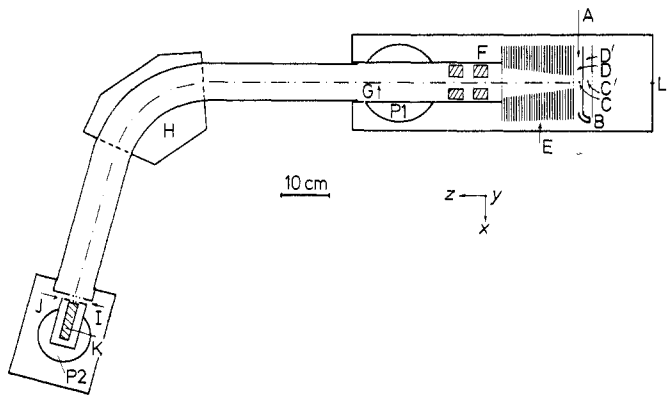

Figure 1. Schematic diagram of the apparatus. A, electron beam; B, Faraday cup; C and C', positions of the gas inlet; D, ionisation chamber: D', reference chamber; E, acceleration section; F, quadrupole optics; G, focal point of the quadrupole optics; H, 60° sector magnetic field mass analyser; I, post-acceleration field; J, focal point of the magnetic field mass analyser; K, Bendix 4700 channeltron; L, normal position of the ionisation gauge; P_1 and P_2, positions of turbomolecular pumps.

(a) For the determination of the target gas density a homogeneous target gas distribution in a large region around the source volume (C in figure 1) is desirable. To achieve this two turbomolecular pumps are used, at positions P1 and P2 in figure 1 (a third turbomolecular pump provides the reference vacuum for the Baratron pressure head). Furthermore, target gas is introduced at positions C and C' (in the y direction 10 cm below the centre of the source volume) by two wide tubes and not a collimated holes structure. Pressure measurements are taken by a Baratron (type 77H–1, range 1 mm Hg, in the y direction 15 cm above the centre of the source volume) and an ionisation gauge (Leybold, type IE37, in the z direction 15 cm away from the centre of the source volume). The background pressure has been reduced to less than 2×10^{-7} Torr and its dependence on additional target gas was investigated (see below).

(b) The energy range of the electron beam has been extended by using two different electron guns: between 0·5 and 2·0 keV the one referred to in Schmidt *et al* 1976a, between 2·0 and 5·0 keV the A61–120W/2 system of AEG–Telefunken. Two pairs of Helmholtz coils were also added to reduce the influence of the Earth's magnetic field on the path of the electron beam (a few mOe along the z direction).

(c) For the purpose of determining its detection efficiency the channeltron was used in two modes, the pulse counting mode and the Faraday cup (current) mode. To meet both requirements, the electrical connections of the channeltron have been installed in such a way that one could switch from the counting mode to the current mode without breaking the vacuum in the apparatus. Figure 2 gives the details. In the counting mode the connections provide for the working conditions described in Schmidt *et al* (1976a). In the current mode the potentials in front of the channeltron ensure that no secondary electrons leave it. The potentials are provided by two blocks of batteries. The block in front of the Cary (model 401) vibrating reed electrometer (A in figure 2) has been highly isolated against ground (resistance larger than $10^{17}\ \Omega$). In the current mode the outer part of the BNC feed-throughs has been used as guarded ring electrode with a potential difference less than 5 mV relative to the central electrode. The resulting leakage current was smaller than 2×10^{-15} A.

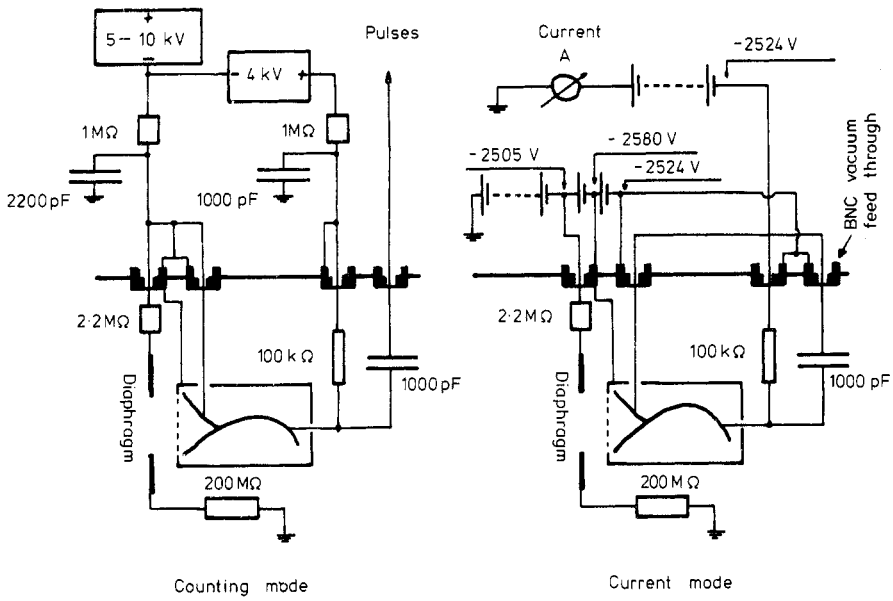

Figure 2. Electrical connections of the channeltron.

(d) The acceleration voltage for the ions (at the end of region E in figure 1) was always set at −2500 V, and the post-acceleration voltages towards the channeltron (in region I) were usually −10 kV, −5 kV and −3·3 kV for singly, doubly and triply charged ions respectively.

2.2. Basic relation

The direct determination of absolute cross sections σ^{n+} for the occurrence of ions with charge n is based on the relation

$$\sigma^{n+} = N_{\text{ion}}^{n+}/(N_e\,\Delta x\,n_v\eta\tau\epsilon)$$

where N_{ion}^{n+} is the number of registered ions per second, N_e is the number of electrons per second in the primary electron beam, Δx is the length of the accepted source volume

(it is assumed that the extension in height (i.e. y direction) of the accepted source volume is larger than the diameter of the electron beam), n_v is the target gas density, η is a factor taking into account the scattering losses of the ion beam, τ is the transmission of the ions through the apparatus and ϵ is the detection efficiency of the channeltron.

2.3. Electron beam

The electron beam traverses the ionisation chamber and is trapped in a curved Faraday cup (10 mm diameter opening). Applying the results of Kollath (1956) to the geometry of this Faraday cup, the number of primary electrons leaving the Faraday cup due to backscattering is less than 2% of the total intensity (for the evaluation of N_e an error of 1% will be used). The Faraday cup is held on a +50 V potential and therefore no secondary electrons can leave the cup (cf Kollath (1956) for the energies of secondaries; in addition, within an error of 1% no change of the electron current I_e could be observed for potentials higher than +40 V on the Faraday cup). As a result of these considerations, the current I_e of the Faraday cup is directly connected with N_e by $N_e = I_e/e_0$ where e_0 is the electron charge. Hereby the possible systematic error of 1% due to backscattering of electrons from the Faraday cup is neglected because it is partly compensated by the backscattering of ions from their detector. The current I_e has been measured with a Keithley electrometer (model 602) and registered using an analogue to digital converter and a counter. An absolute error of 2% (declaration of manufacturer) has been attributed to the determination of I_e.

An interesting quantity is the diameter of the electron beam. For currents less than 10^{-8} A and in the centre of the ionisation chamber it has been measured to be 4·3 mm at 0·5 keV, 3·3 mm at 2·0 keV and 2·8 mm at 5·0 keV. Here and in the following the diameter refers to that value in which 99% of the total intensity is concentrated.

2.4. Source volume

The accepted source volume is defined as that region in the ionisation chamber from which all ions of correct e/m value traverse the apparatus and reach the detector. Following the paths of individual ions it can be shown that the length x is determined by the length Δx of the rectangular opening in the gold foil at the beginning of the acceleration section. The latter is given by $\Delta x = (0{\cdot}975 \pm 0{\cdot}005)$ cm. In the z direction the accepted source volume extends over the whole region of the ionisation chamber provided the electron beam does not hit the walls of it. The only critical quantity of the accepted source volume is its height Δy because limitations could occur due to the height (14 mm) of the diaphragm opening in front of the channeltron. Information about the height Δy is connected directly with that about transmission τ of the apparatus. In order to get information on these quantities, the counting rate of ions (with fixed e/m value) has been observed as a function of the y position of the electron beam in the ionisation chamber. The decrease of the counting rate by 1% and the known diameter of the electron beam yielded $\Delta y = 5{\cdot}0$ mm which is always larger than the diameter of the electron beam.

2.5. Target gas density

In order to avoid ion–molecule reactions, the pressure dependence of all singly and doubly charged ions has been examined. The reduction of the counting rate was found

to be smaller than 1% for the target gas pressures lower than 2×10^{-5} Torr for He, Ne, Ar and 8×10^{-6} Torr for Kr, Xe, respectively. In all cross section measurements, the target gas pressure was kept below these values, i.e. $\eta = 1{\cdot}00$. For the measurement of such low target gas pressures, the Baratron could not be used directly, but a calibrated ionisation gauge (Leybold IE 37). To determine the true target gas pressure the influence of the target gas on the background pressure has been investigated. The peaks of H_2O^+, N_2^+ and O_2^+ and a region without structure at mass 32 have been selected. No systematic change of intensity (within less than 5%) could be observed for these background components for target gas pressures up to 2×10^{-5} Torr. This result and the low background of 2×10^{-7} Torr justify, for a homogeneous pressure distribution, the following relation between the pressures p (in Torr) measured with the Baratron and the divisions I of the ionisation gauge:

$$p_t = p - p_{BG} = f_t(I - I_{BG}).$$

In this expression no index refers to measurements with target gas and background, BG refers to those for background alone and t stands for target gas. f_t is the calibration factor which depends on the selected target gas, the specific ionisation gauge and the surroundings of that gauge. When f_t is determined, the target gas density n_v (cm^{-3}) is

$$n_v = 3{\cdot}535\times10^{16}(T_0/T)f_t(I - I_{BG})$$

where the target gas temperature (room temperature 295 ± 2 K) is denoted by T and $T_0 = 273$ K. The factors f_t were determined for at least ten different pressures within the accessible region of both instruments; the lower limit at 2×10^{-5} Torr was given by the Baratron, the higher limit was set by the safety current of the ionisation gauge. The latter corresponds to different pressure values for each rare gas, but in all cases the 10^{-3} Torr full-scale range of the Baratron was reached in order to have not more than approximately 1% absolute error for the pressure value of the Baratron (declaration of the manufacturer). This procedure yielded for each target gas a set of calibration factors f_t which are equal within an error of less than 2%. Due to the ionisation mechanism itself these calibration factors f_t should be valid also for lower gas pressures. This gives, together with the linearity (better than 0·5%) of the ionisation current amplifier, the required extension of the absolute determination of target gas pressures around or below 10^{-5} Torr. The error of this calibration (statistical error, error of linearity and error of influence of different temperatures (±2 °C deviations)) has been determined to 2%. The pressure readings of the ionisation gauge and of the Baratron were monitored using a voltage–frequency converter and a counter.

The Baratron head was always used at its regulated temperature of 49 °C, i.e. the difference between the temperature at the Baratron head ($T_I = 49$ °C) and in the vacuum tank ($T_{II} = 22$ °C) must be taken into consideration because it can produce differences in pressure or target gas density at the Baratron head (p_I, n_I) and in the vacuum tank (p_{II}, n_{II}). Only in the 1 Torr region does $p_I = p_{II}$. This situation changes for lower pressures ($<10^{-3}$ Torr) because there thermomolecular flow will occur until the steady state with $p_I/p_{II} = (T_I/T_{II})^{1/2}$ is reached. The change from high to low pressures is described by the Liang equation (compare Bennett and Tompkins 1957). However, this result is valid only when an aperture is used as a temperature interface (Edmonds and Hobson 1965). For a tube interface the correction depends on the geometry of those parts of the connection over which the temperature change occurs. For the type of Baratron used in our experiment, there are now available three experimental determinations of the required correction: 1·0% (Bromberg 1969), 2·6%

(Baldwin and Gaerttner 1973) and 2·0% (Blaauw *et al* 1980). From these results we applied a systematic correction of −2·0% to the reading of our Baratron.

The statement that the calibrated ionisation gauge also gives the target gas pressure in the region of the source volume requires an investigation of the homogeneity of the target gas distribution in the relevant region. This has been done by mounting the Baratron pressure head at various positions on the apparatus while a reference ionisation gauge is kept at a fixed position. Four different mountings of the Baratron pressure head could be used, the first at its normal position (15 cm above point C in figure 1), the second and third at those of the IE37 ionisation gauge (position L in figure 1) where in one case a tube gave a direct connection between the middle of the simulated source volume C′ and the pressure head, and the fourth at a position half way toward the turbomolecular pump at position F in figure 1. At this last position, the pressure dropped by almost a factor of two. But all three other mountings in the relevant regions between the ionisation chamber and the normal positions for the Baratron and IE37 ionisation gauge gave the same results within an error of 6%. This means that the open space of this region is shielded quite well against the influence of the turbomolecular pump at position P1 by the numerous diaphragms of the acceleration section. The error of 6% is governed by the error of reproducibility of the reference ionisation gauge when it has been switched off between two measurements to change the connection of the Baratron pressure head. Therefore a possible error of only 3% is attributed to deviations from a homogeneous target gas distribution in the relevant region.

2.6. Transmission

The transmission of the ions from the target volume to the channeltron is determined by two factors: losses due to copper meshes and possible losses due to insufficient image properties of the quadrupole lenses and the magnetic field mass analyser.

With an additional movable mesh behind the acceleration section the transmission of ions at one copper mesh has been determined to be $0{\cdot}915 \pm 0{\cdot}010$. Within the error bars, no deviation from this value could be found for ions with energies between 300 eV and 2·5 keV. This value is therefore used at all four copper meshes, giving a transmission factor $\tau_M = 0{\cdot}70$ with a relative error of about 2·5%.

By varying the value of the homogeneous electric field (usually 25 V cm^{-1}) in the ionisation chamber D of figure 1 (within 15 V cm^{-1} and 40 V cm^{-1}, the limits are determined by the deflection of the electron beam and the geometrical design of the ionisation chamber and Faraday cup) the ion counting rate was constant to within less than 1%. This means that all ions from the real source volume enter the acceleration region. Possible losses on their subsequent path can only be due to insufficient image properties which may result in a transmission τ_0 less than unity. As described by Schmidt *et al* (1976a) the profile of the ion beam was observed with a channel plate and a connected phosphorous screen and its size has been compared with theoretical estimates. The agreement is good and allows the statement of a 100% transmission (apart from losses at the copper meshes), i.e. $\tau_0 = 1{\cdot}00$. This value is also supported by the earlier measurement of the transmission through the magnetic field mass analyser (Schmidt *et al* 1976a) which gave $1{\cdot}00 \pm 0{\cdot}06$). In that experiment the transmission error was governed by the error of reproducibility of equal target gas pressure measured with an ionisation gauge at the high pressure region of a collimated holes structure used as a gas inlet. As already mentioned, the determination of the height Δy of the accepted

source volume also confirms a 100% transmission. On the basis of the above discussion we shall use $\tau_0 = 1{\cdot}00$ with an estimated error of 2%.

2.7. Detection efficiency

As described above, the detection efficiency ϵ of the channeltron has been determined using the experimental arrangement of figure 2 without breaking the vacuum. The results of the counting and the current mode (each corrected for background contributions) give ϵ. The counting mode could be used up to 1×10^4 counts/s (the limit of linearity of the channeltron), the current mode required at least 10^6 ions/s. To accomplish this the intensity of the electron beam was increased from some 10^{-10} A to some 10^{-7} A. In this case the absence of deviations from the linear response between the number of ions and the intensity of the electron beam must be ensured. These measurements have therefore been made using the electron beam at 5 keV energy, in which case at the maximum current the diameter is enlarged by only 0·3 mm. The Cary electrometer was used in the rate-of-charge mode for the current measurement, which allows an absolute accuracy of 0·25% for the ion current value. Typical ion currents were between 10^{-13} A and 10^{-12} A. The resulting error for the detection efficiency ϵ is 2%. It contains the absolute error of the Cary electrometer and the errors of the ion

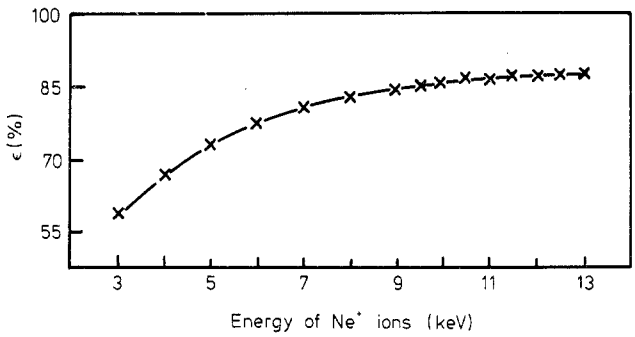

Figure 3. Detection efficiency ϵ of our channeltron for Ne^+ ions.

Table 1. Experimental values for ionisation cross sections σ^+ and ratios $R_1 = \sigma^{2+}/\sigma^{1+}$ and $R_2 = \sigma^{3+}/\sigma^{2+}$ as functions of electron impact energy E.

Rare gas	E(keV)	σ^+(M barn)	R_1(%)	R_2(%)
Helium	0·5	16·5	0·570	
	0·7	14.4	0·561	
	1·0	12·0	0·480	
	1·5	8·21	0·447	
	2·0	6·93	0·405	
	2·5	5·55	0·415	
	3·0	4·90	0·394	
	3·5	4·24	0·375	
	4·0	3·85	0·363	
	4·5	3·46	0·360	
	5·0	3·12	0·359	

Table 1. (continued)

Rare gas	E(keV)	σ^+(Mbarn)	R_1(%)	R_2(%)
Neon	0·5	46·8	4·62	6·08
	0·7	37·4	4·28	6·22
	1·0	29·4	4·06	6·08
	1·5	22·0	3·64	6·20
	2·0	17.2	3·50	6·20
	2·5	14·7	3·31	6·27
	3·0	12·6	3·20	6·30
	3·5	11·2	3·12	6·56
	4·0	10·0	3·12	6·54
	4·5	9·10	3·13	6·69
	5·0	8·40	3·14	6·73
Argon	0·5	123·0	5·47	10·5
	0·7	97·2	5·45	13·4
	1·0	75·5	5·66	14·1
	1·5	56·4	5·41	18·3
	2·0	46·3	5·09	22·4
	2·5	38·7	5·15	22·9
	3·0	33·0	5·12	22·7
	3·5	29·5	5·22	24·1
	4·0	26·2	5·25	23·6
	4·5	24·0	5·15	25·6
	5·0	22·0	5·19	25·9
Krypton	0·5	190·0	5·20	38·0
	0·7	140·0	5·27	44·7
	1·0	107·0	6·31	48·4
	1·5	76·9	6·84	54·7
	2·0	59·7	7·68	54·1
	2·5	48·1	7·78	57·2
	3·0	41·8	7·90	59·0
	3·5	36·3	8·01	60·4
	4·0	32·5	8·12	60·2
	4·5	29·5	8·20	60·8
	5·0	26·8	8·25	61·3
Xenon	0·5	212·0	10·9	48·5
	0·7	154·0	10·8	48·4
	1·0	121·0	12·7	45·9
	1·5	90·7	14·1	45·5
	2·0	73·2	14·9	42·2
	2·5	60·8	15·1	43·3
	3·0	51·6	15·7	42·5
	3·5	45·4	15·7	42·2
	4·0	41·0	15·8	42·4
	4·5	36·9	16·2	42·1
	5·0	33·8	16·1	42·2

current and leakage current measurement. Back scattering of ions from the channeltron surface is small enough to be neglected. This has been controlled by comparing the results of a Faraday cup with a suitable geometry with the results of the channeltron in the current mode.

Within the experimental error, the detection efficiency ϵ of 10 keV ions was equal for all rare gases and, furthermore, no difference could be found for the detection

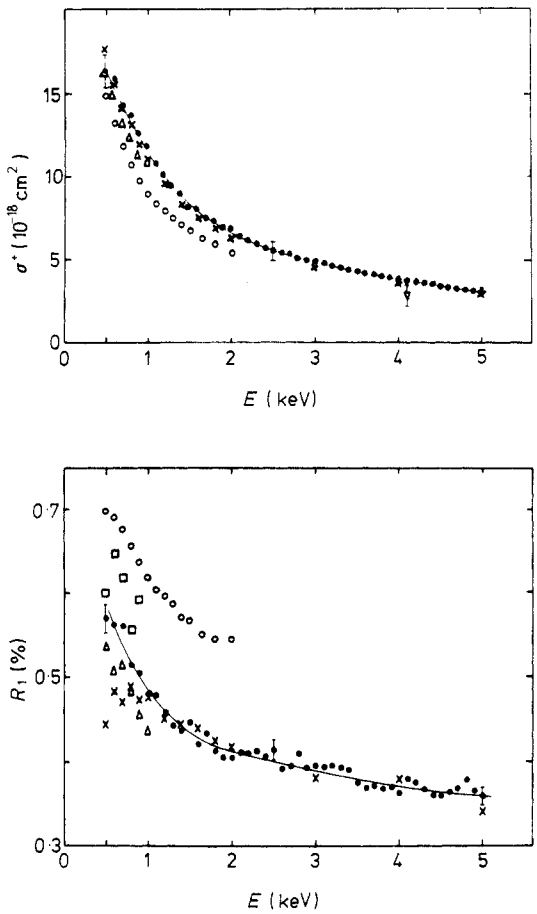

Figure 4. Electron impact ionisation cross section σ^{1+} (with representative 6% error bars at three energies) and ratio $R_1 = \sigma^{2+}/\sigma^{1+}$ (with 2·5% error bars at three points) for He as a function of electron impact energy. The smooth curve is a guide through our experimental data (points). Other experimental data: □ Harrison (1966) (from Kieffer and Dunn (1966), figure 32); × Schram *et al* (1966); △ Adamczyk *et al* (1966); ○ Gaudin and Hagemann (1967); ▽ Shchemelinin and Andreev (1976).

efficiency of doubly and triply charged ions when their velocity was equal to that of the 10 keV singly charged ions. For the evaluation of the cross sections σ^{n+} the individually determined values of ϵ have been used. As an example, figure 3 shows the detection efficiency ϵ for Ne^+ ions for the channeltron which has been already used for several years.

Finally, it should be mentioned that this channeltron had a constant surface sensitivity: when the ion peak was scanned as a function of the current of the magnetic field mass analyser, the variations of the counting rate in the region of the peak plateau were less than 0·2%.

2.8. Measurement procedure

Before, after, and from time to time also during each measurement on one of the rare

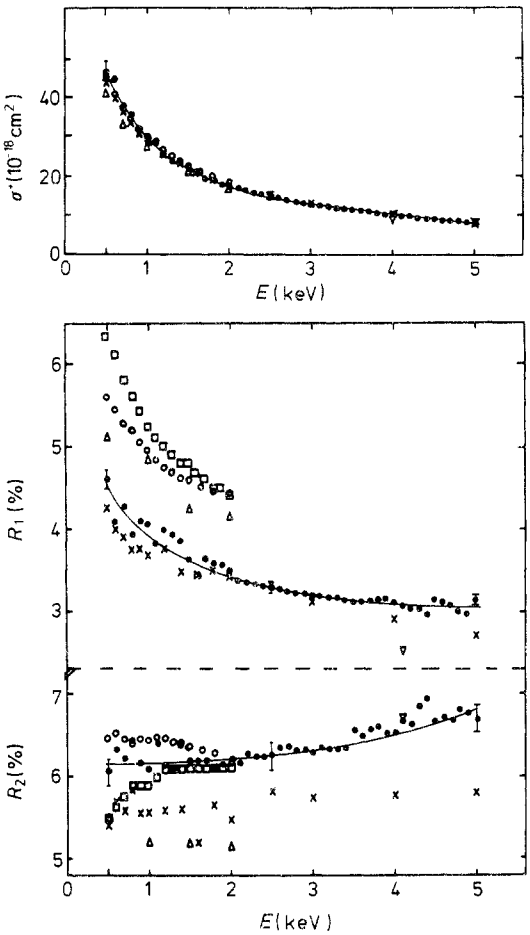

Figure 5. Electron impact ionisation cross section σ^{1+} and ratios $R_1 = \sigma^{2+}/\sigma^{1+}$ and $R_2 = \sigma^{3+}/\sigma^{2+}$ for Ne as function of electron energy. For further details see the caption of figure 4. Other experimental data: □ Ziesel (1965); × Schram *et al* (1966); △ Adamczyk *et al* (1966); ○ Gaudin and Hagemann (1967); ▽ Shchemelinin and Andreev (1976).

gases, the IE37 ionisation gauge was calibrated against the Baratron. During all measurements the ionisation gauge was kept running continuously. For each energy setting of the electron beam, the beam diameter and the correct passage of the electron beam through the centre of the accepted source volume were determined. At each electron beam energy and at constant target gas pressure the counting rate of singly and doubly charged ions were registered as functions of the current in the magnetic field mass analyser (at higher electron current the same was done for the counting rate of doubly and triply charged ions). From these data, the ion counting rate N_{ion}^{n+} was evaluated as the mean value in the plateau minus the background. For Kr only the plateau of the isotope Kr^{86} was used, for Xe only that of Xe^{136}. The detection efficiency of the channeltron was determined at the end of these measurements on one rare gas for all energies of the electron beam. This procedure gave all quantities necessary to evaluate σ^{n+} and the ratios $R_1 = \sigma^{2+}/\sigma^{1+}$ and $R_2 = \sigma^{3+}/\sigma^{2+}$ with the smallest possible errors.

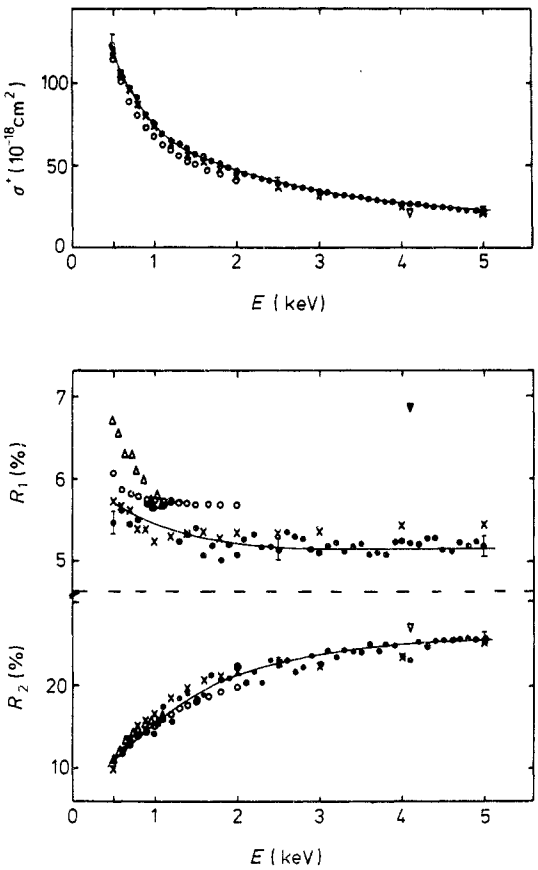

Figure 6. Electron impact ionisation cross section σ^{1+} and ratios $R_1 = \sigma^{2+}/\sigma^{1+}$ and $R_2 = \sigma^{3+}/\sigma^{2+}$ for Ar as function of electron energy. For further details see the caption of figure 4. Other experimental data: × Schram (1966); ○ Gaudin and Hagemann (1967); △ Okudaira *et al* (1970); ▽ Shchemelinin and Andreev (1976).

3. Results

For all rare gases the ionisation cross sections σ^{n+} with $n = 1$, 2 and 3 and the ratios $R_i = \sigma^{(i+1)+}/\sigma^{i+}$ with $i = 1$, 2 have been determined for energies of the electron beam ranging from 0·5 keV to 5 keV. For He, Ne and Ar steps of 100 eV were taken, for Kr and Xe larger steps. For these larger steps, table 1 gives a compilation of the data for all rare gases (for He, Ne and Ar the data at the other energies are available from the authors on request).

3.1. Discussion of errors

The statistical error of the ion counting rates is about 0·2% (with the exception of He^{2+} where it reaches 0·5%). The individual errors of all quantities which contribute to the evaluation of σ^+ have been quoted above. Their combined RMS value gives 6%. For the

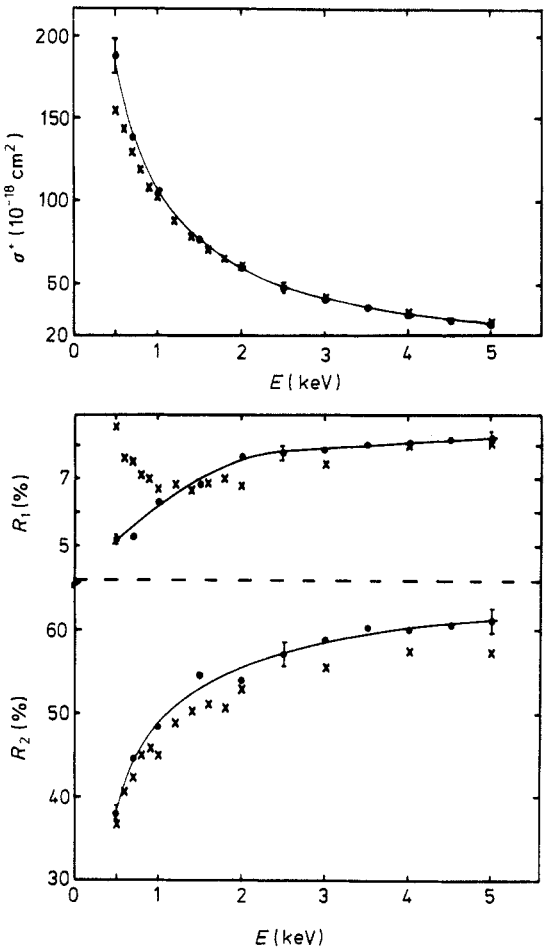

Figure 7. Electron impact ionisation cross section σ^{1+} and ratios $R_1 = \sigma^{2+}/\sigma^{1+}$ and $R_2 = \sigma^{3+}/\sigma^{2+}$ for Kr as function of electron energy. For further details see the caption of figure 4. Other experimental data: × Schram (1966).

ratios R_i only the error of the transmission τ_0 and the error of possible charge discrimination on the copper meshes can contribute in addition to the statistical error. This gives about 2·5%. Schmidt *et al* (1976a) quoted for the ratio R_1 an inherent error of 7%. The present investigation explains most of that inherent error as a consequence of the fact that in that work the post-acceleration voltage was not adapted correctly (−7 kV for singly and −5 kV for doubly charged ions). This means that unequal detection efficiencies are possible for singly and doubly charged ions, depending critically on the individual efficiency curve of the channeltron.

In order to include possible (and as yet unknown) errors, and to take into account the possibility of systematic deviations rather than the pure statistical RMS combination of all individual error contributions, we shall quote our results with an additional error of 2·5% for the ratios R_i and of 4% for σ^{1+} respectively. This gives a total error of 10% for σ^{1+} and of 5% for the ratios R_1 and R_2. The errors in the energy value of the electron beam are 0·3% below 2 keV and 2% above 2 keV.

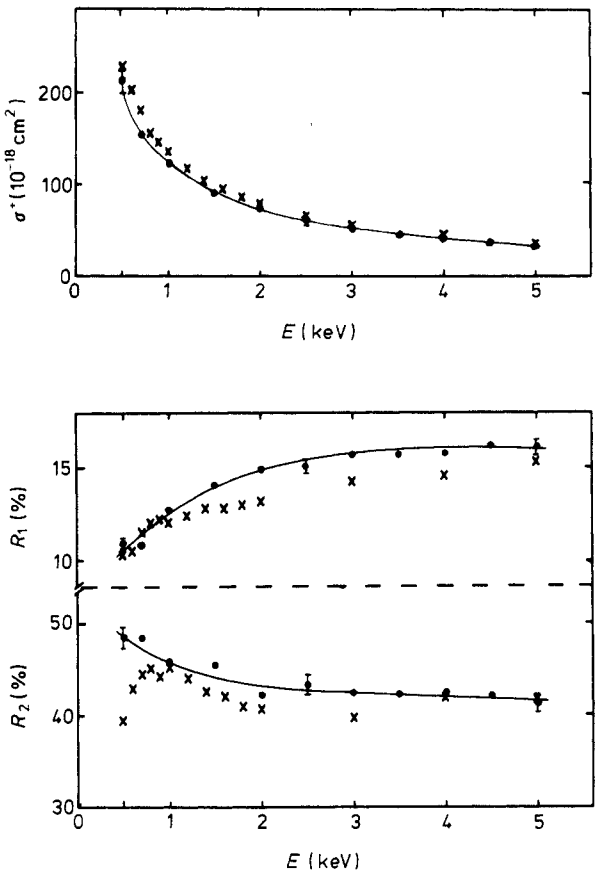

Figure 8. Electron impact ionisation cross section σ^{1+} and ratios $R_1 = \sigma^{2+}/\sigma^{1+}$ and $R_2 = \sigma^{3+}/\sigma^{2+}$ for Xe as function of electron energy. For further details see the caption of figure 4. Other experimental data: × Schram (1966).

4. Comparison with other experimental data

It would be too confusing to compare our results with all available data. Therefore, the following selection has been made.

(a) Only those data are included in our figures which are based on the direct determination of σ^{n+} or R_i, i.e. experiments giving $\sigma_{\text{gross ion}}$ are not taken into account (for these data see the review article by Kieffer and Dunn 1966).

(b) When data for σ^{n+} or R_i are available only for energies below 600 eV electron impact energy, they have been omitted because our data are above 500 eV.

(c) Due to the new results in quasi-photon impact experiments by Wight and van der Wiel (1976) and the discussion therein, the electron impact data of van der Wiel *et al* (1969) and El-Sherbini *et al* (1970) have been omitted. Also, the results of Stanton and Monahan (1960) and of Stuber (1965) are not shown because they need a correction for the energy dependence of the multiplier efficiency, in the counting mode as well as in the current mode.

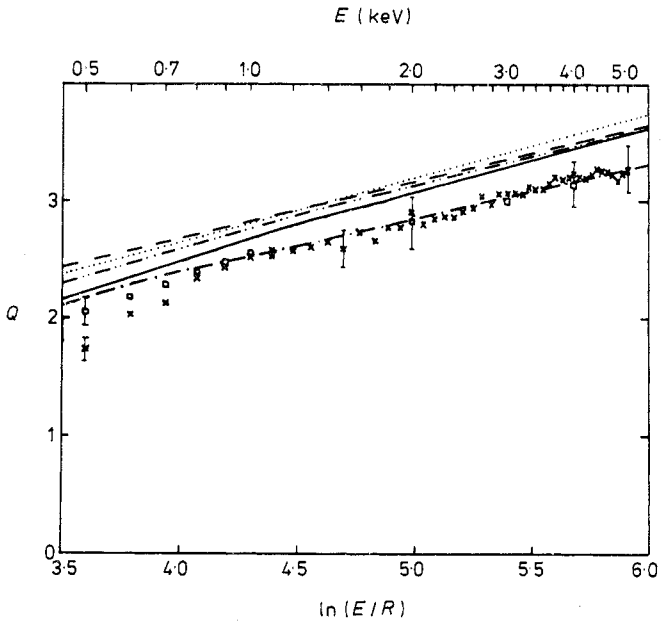

Figure 9. Fano–Bethe plot for the total ionisation cross section of He represented as $Q = \sigma_{ion}E/(4\pi a_0^2 R)$. Our experimental data are shown as crosses with representative 6% error bars at three energies. The open squares (again with error bars at some selected energies) are extracted from the average experimental ionisation cross sections derived by de Heer and Jansen (1977). Theoretical calculations: · · · Bell and Kingston (1969) (results for length form (L) and velocity form (V) of the matrix element cannot be resolved in the figure); —·— Economides and McDowell (1969) (velocity form); –··– Economides and McDowell (1969) (length form) (the data of McGuire (1971) also follow this curve); – – – Kim and Inokuti (1971) (Bethe approximation); —— Kim and Inokuti (1971) (Born approximation with free electron exchange).

In figures 4 to 8, our data are compared with those of the other experiments. The details can be seen directly from these figures. As a general result it follows that our data agree very well with those of Schram *et al* (1966) and Schram (1966).

As part of their study on total cross sections for electron scattering on rare gases, de Heer and Jansen (1977) and de Heer *et al* (1979) also quote average experimental ionisation cross sections σ_{ion} which have been derived by a specific weighting procedure of all hitherto existing experimental data. Our results for σ_{ion} are compared with these average values in the Fano–Bethe plot representation in figures 9 to 13. The agreement is good. The worst comparison case is Ar for energies above 1 keV where our values are systematically larger; nevertheless, the two data sets still have overlapping error bars.

5. Comparison with theory

The best basis for the analysis of the data from theoretical point of view is given in the Fano–Bethe plot, i.e. $Q = \sigma_{ion}E/(4\pi a_0^2 R)$ is plotted as function of $\ln(E/R)$ where E is the energy of the electron beam and R the Rydberg energy. This representation allows

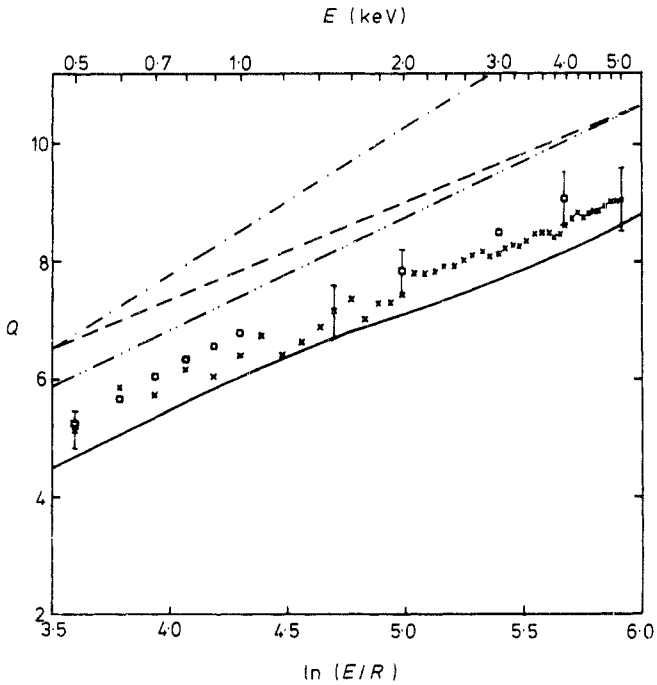

Figure 10. Fano–Bethe plot for the total ionisation cross section of Ne. For further details see the caption of figure 9. □ de Heer *et al* (1979). Theoretical calculations: –··– McGuire (1971); –·– Wallace *et al* (1973); – – – Saxon (1973); —— Knapp and Schulz (1974).

the following parametrisation (Inokuti 1971, Kim and Inokuti 1971)

$$Q = M_i^2 \ln(E/R) + C_i + \gamma_i R/E$$

this expression gives the Born asymptote. For high energies E the γ_i term can be neglected and this yields the Bethe asymptote. The parameters are related to data of the optical oscillator strength and to properties of the ground-state wavefunction. Exchange corrections can also be included in this parametrised expression by replacing γ_i by the corresponding quantity γ_i^{exch}.

Figures 9 to 13 show the Fano–Bethe plots for the rare gases. Our experimental data are displayed with 6% error bars, i.e. according to our error discussion the whole curve is allowed to shift by about ±4%. The fluctuations in our experimental values are of experimental origin (temperature fluctuations, error of the pressure calibration, position of the electron beam which is reflected also in the error of the transmission τ_0, calibration error for electron beam current and energy). Also shown (open squares) is the region of average experimental ionisation cross sections σ_{ion} as evaluated by de Heer and Jansen (1977) and de Heer *et al* (1979). In our figures, theoretical cross sections σ_{ion} are also given. Semiclassical approaches (e.g. Gryzinski 1965) and Born calculations with hydrogenic wavefunctions (e.g. Omidvar *et al* 1972) have been omitted.

For the case of He, the calculations of Bell and Kingston (1969), Economides and McDowell (1969) and McGuire (1971) are direct calculations of σ_{ion}. The data of Kim and Inokuti (1971) come from sum rule considerations. Their two curves clearly

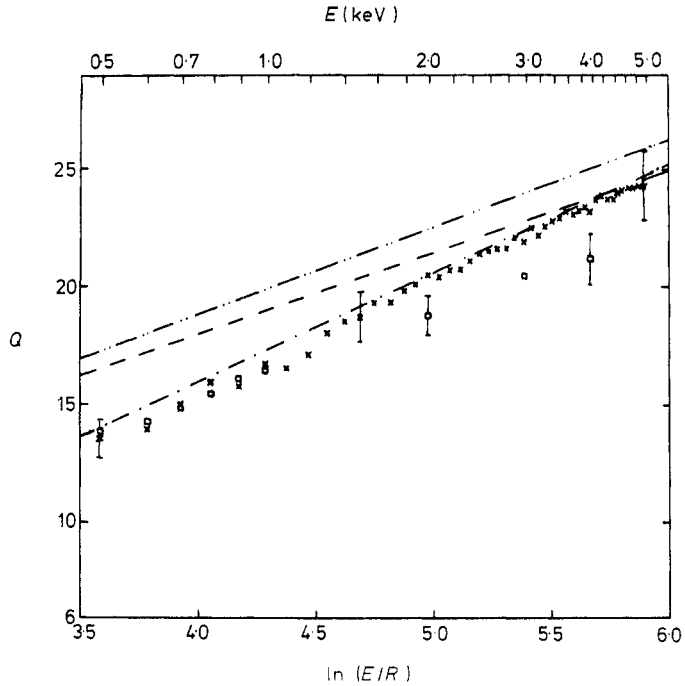

Figure 11. Fano–Bethe plot of the total ionisation cross section of Ar. For further details see the caption of figure 9. □ de Heer *et al* (1979). Theoretical calculations: ·-·-· McGuire (1971); –·– Wallace *et al* (1973); --- Kim *et al* (1973) and also Eggarter (1975) (slightly higher than Kim *et al* 1973).

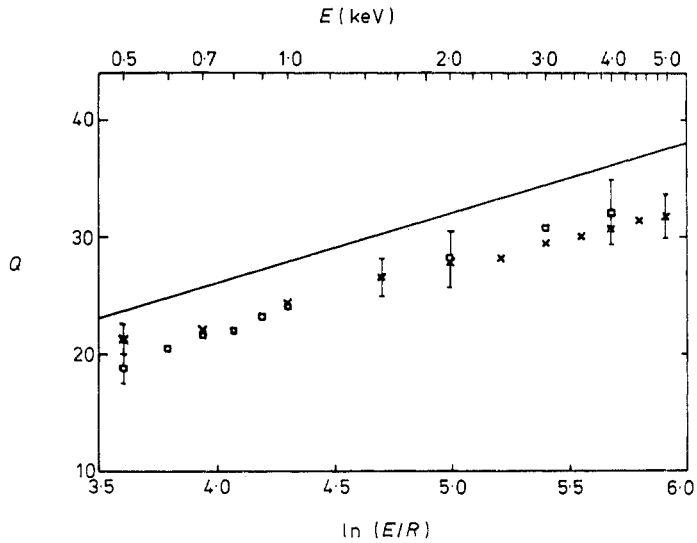

Figure 12. Fano–Bethe plot of the total ionisation cross section of Kr. For further details see the caption of figure 9. □ de Heer *et al* (1979); full curve, calculation of McGuire (1977).

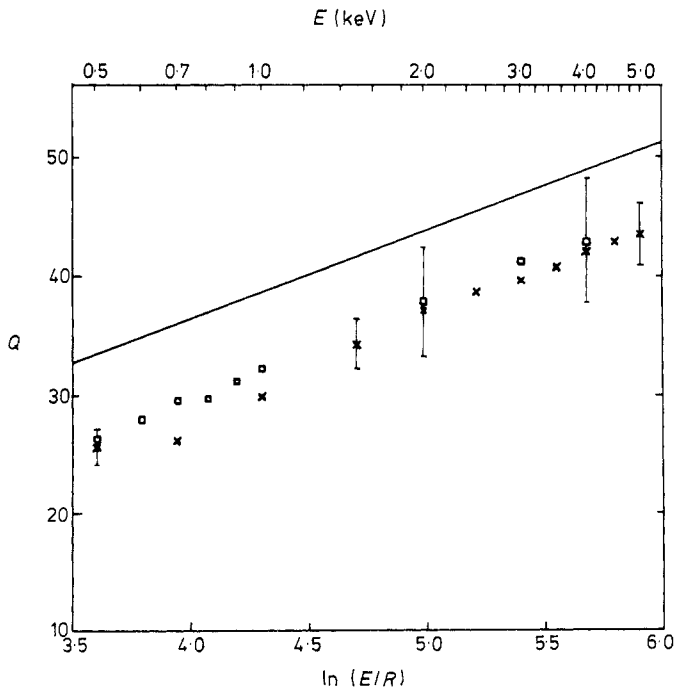

Figure 13. Fano–Bethe plot of the total ionisation cross section of Xe. For further details see the caption of figure 9. □ de Heer *et al* (1979); full curve, calculation of McGuire (1977).

demonstrate the influence of the γ_i term in the Born approximation (with free electron exchange) with respect to the Bethe asymptote.

Instead of σ_{ion} each σ^{n+} can be displayed in a Fano plot. This is of special interest for σ^{2+} of He because the experiment of Schram *et al* (1966) gave for this case a negative slope which is in contradiction to the interpretation of M_i^2 as the dipole matrix element squared for ionisation (see also van der Wiel and Wiebes 1971). When our σ^{2+} data for He are presented in a Fano–Bethe plot, a positive slope is achieved: $M_i^2(\text{He}^{2+}) = (3 \pm 1) \times 10^{-3}$.

For the case of Ne, the curves of McGuire (1971), Wallace *et al* (1973) (only single ionisation) and Knapp and Schulz (1974) come from direct calculations of the ionisation cross section. Knapp and Schulz (1974) have taken into account the exchange effects between the ejected electron and the electrons which are bound in the ion. The Bethe asymptote for σ_{ion} has been derived by Saxon (1973) on the basis of sum rule considerations. It can be expected that this curve is lowered and changes its slope when the γ_i term (for the Born asymptote and taking exchange effects into account) would be included (compare the calculation of Knapp and Schulz (1974) which includes both effects and where the curve changes slope at around 1 keV).

In Ar, the data of E J McGuire (1979, private communication) and Wallace *et al* (1973) (only single ionisation) again represent direct calculations. Kim *et al* (1973) and Eggarter (1975) evaluated the Bethe asymptote for σ_{ion}. Here our data are already very close to this curve of the Bethe asymptote for high energies. For lower energies, the inclusion of the γ_i term will probably change this theoretical curve towards smaller values.

In Kr and Xe, comparison can be made only with the direct calculation of McGuire (1977). Our plotted experimental data are systematically lower than the true experimental values by about 1% or 2% for Kr or Xe, respectively, because only charge states up to $n = 3$ are included.

In conclusion, the data presented in this paper yield total ionisation cross sections σ_{ion} which are in good agreement with the average experimental ionisation cross sections evaluated by de Heer and Jansen (1977) and by de Heer *et al* (1979). The cross sections σ_{ion} for He, Ne and Ar are close to theoretical calculations based on sum rules (Kim and Inokuti 1971, He; Kim *et al* 1973 and Eggarter 1975, Ar) or on direct calculations using good wavefunctions (Knapp and Schulz 1974, Ne) provided exchange effects are taken into account. The direct calculation of McGuire (1971, 1977, 1979 private communication) gives results for all rare gases which are systematically larger (typically about 14% at 2 keV electron energy) with respect to the experimental data. Inclusion of exchange effects lowers theoretical cross sections. Therefore direct calculations with exchange taken into account are highly desirable.

Acknowledgments

The authors thank Dr W Mehlhorn for support and his continuing interest, A Koch for his contribution on some of the measurements, Dr F de Heer for sending the average experimental ionisation cross sections prior to publication, Dr E J McGuire for kindly communicating his numerical results and Dr G Messer for helpful discussions. Financial support by the Deutsche Forschungsgemeinschaft is gratefully acknowledged.

References

Adamczyk B, Boerboom A J H, Schram B L and Kistemaker J 1966 *J. Chem. Phys.* **44** 4640–2
Baldwin G C and Gaerttner M R 1973 *J. Vac. Sci. Technol.* **10** 215–7
Bell K L and Kingston A E 1969 *J. Phys. B: Atom. Molec. Phys.* **2** 1125–30
Bennett M J and Tompkins F C 1957 *Trans. Faraday Soc.* **53** 185–92
Blaauw H J, Wagenaar R W, Barends D H and de Heer F J 1980 *J. Phys. B: Atom. Molec. Phys.* **13** 359–76
Bransden B H and McDowell M R C 1969 *J. Phys. B: Atom. Molec. Phys.* **2** 1187–201
——1970 *J. Phys. B: Atom. Molec. Phys.* **3** 29–33
Bromberg J P 1969 *J. Vac. Sci. Technol.* **6** 801–8
Economides D G and McDowell M R C 1969 *J. Phys. B: Atom. Molec. Phys.* **2** 1323–31
Edmonds T and Hobson J P 1965 *J. Vac. Sci. Technol.* **2** 182–97
Eggarter E 1975 *J. Chem. Phys.* **62** 833–47
El-Sherbini Th M, van der Wiel M J and de Heer F J 1970 *Physica* **48** 157–64
de Heer F J and Jansen R H J 1977 *J. Phys. B: Atom. Molec. Phys.* **10** 3741–58
de Heer F J, Jansen R H J and van der Kaay W 1979 *J. Phys. B: Atom. Molec. Phys.* **12** 979–1002
de Heer F J, Wagenaar R W, Blaauw H J and Tip A 1976 *J. Phys. B: Atom. Molec. Phys.* **9** L269–74
Gaudin A and Hagemann R 1967 *J. Chim. Phys.* **64** 1209–21
Gryzinski M 1965 *Phys. Rev.* A **138** 336–58
Harrison H 1966 *PhD Thesis* (Washington, DC: The Catholic University of America Press)
Inokuti M 1971 *Rev. Mod. Phys.* **43** 297–347
Inokuti M, Kim Y K and Platzmann R L 1967 *Phys. Rev.* **164** 55–61
Kieffer L J and Dunn G H 1966 *Rev. Mod. Phys.* **38** 1–35
Kim Y K and Inokuti M 1971 *Phys. Rev.* **3** 665–78
Kim Y K, Naon M and Cornille M 1973 *Argonne Nat. Lab. Report* ANL 8060 14–23
Knapp E W and Schulz M 1974 *J. Phys. B: Atom. Molec. Phys.* **7** 1875–90
Kollath R 1956 *Handbuch der Physik* vol 21, ed S Flügge (Berlin: Springer) pp 232–303

McGuire E J 1971 *Phys. Rev.* A **3** 267–79
—— 1977 *Phys. Rev.* A **16** 62–72
Okudaira S, Kaneko Y and Kanomato I 1970 *J. Phys. Soc. Japan* **28** 1536–41
Omidvar K, Kyle H L and Sullivan E C 1972 *Phys. Rev.* A **5** 1174–87
Saxon R P 1973 Phys. Rev. A **8** 839–49
Schmidt V, Sandner N and Kuntzemüller H 1976a *Phys. Rev.* A **13** 1743–47
Schmidt V, Sandner N, Kuntzemüller H, Dhez P, Wuilleumier F and Källne E 1976b *Phys. Rev.* A **13** 1748–55
Schram B L 1966 *Physica* **32** 197–208
Schram B L, Boerboom A J H and Kistemaker J 1966 *Physica* **32** 185–96
Shchemelinin S G and Andreev A P 1976 *Sov. Phys.-Tech. Phys.* **20** 941–3
Smith P T 1930 *Phys. Rev.* **36** 1293–302
Stanton H E and Monahan J E 1960 *Phys. Rev.* **119** 711–5
Stuber F A 1965 *J. Chem. Phys.* **42** 2639–43
Wallace S J, Berg R A and Green A E S 1973 *Phys. Rev.* A **7** 1616–29
van der Wiel M J, El-Sherbini Th M and Vriens L 1969 *Physica* **42** 411–20
van der Wiel M J and Wiebes G 1971 *Physica* **54** 411–24
Wight G R and van der Wiel M J 1976 *J. Phys. B: Atom. Molec. Phys.* **9** 1319–27
Ziesel J P 1965 *J. Chim. Phys.* **62** 328–35